Determination of the water retention curve from drying experiments using infrared thermography: A preliminary study

Michele Bianchi Janetti [a, *], Luigi P.M. Colombo [b], Fabian Ochs [a], Wolfgang Feist [a, c]

[a] University of Innsbruck, Institute of Structural Engineering and Material Sciences, Unit for Energy Efficient Buildings, Technikerstr. 13, 6020 Innsbruck, Austria
[b] Dipartimento di Energia, Politecnico di Milano, via Lambruschini 4, 20156 Milan, Italy
[c] Passivhaus Institut Dr. Wolfgang Feist, Rheinstr. 44/46, 64283 Darmstadt, Germany

A method is proposed for experimental determination of the water retention curve from drying tests performed on capillary active materials. Non-destructive techniques (gravimetric analysis, infrared thermography) are employed for measuring water content, drying rate and surface temperature during time for a set of material samples. The surface relative humidity is calculated from the measured data through analytical procedure. Hence, assuming uniform water content distribution inside the samples, which applies if the mass transfer Biot number is small enough, the relation between relative humidity and water content is derived. This relation represents the water retention curve for the considered transient desorption behavior and, as shown in previous studies, it may deviate from the trend measured through steady state experiments.

The proposed method differs substantially from other ones commonly employed to the same aim. It is useful for investigation of the so called dynamic effects, recently observed by other authors in the hygrothermal behavior of construction materials. For a first test, calcium silicate specimens are employed and the results are compared with those reported in the literature. An error propagation analysis is also included.

Keywords: Water retention curve, Capillary active materials, Calcium silicate Infrared thermography, Dynamic effects

1. Introduction

Deep knowledge of heat, vapor and liquid water transfer in construction materials is a prerequisite for the proper design of building components. This is particularly relevant in cases where an existing building is refurbished by applying internal insulation [1]. For this reason, a great effort in both numerical modeling and experimental research has been recently made on this topic by numerous authors [2–9]. The purpose of this work is to extend the present knowledge by investigating the drying behavior of calcium silicate, the importance of which as capillary active thermal insulation material has been already shown in the literature [10,11].

A new method is proposed for experimental determination of the water retention curve in both the hygroscopic and super-hygroscopic ranges, based on non-destructive measurements and analytical procedure. The proposed method is less time consuming and differs in a substantial way from the other ones used for the same purpose.

Article history:
Received 21 June 2016
Received in revised form 11 November 2016
Accepted 27 December 2016

2. State of the art

The water retention curve describes the capability of a porous material to retain water inside its air cavities and represents an important input for transient modeling of heat and moisture transfer. It can be expressed as a relation between the local water content and the relative humidity or, alternatively, the capillary pressure (Fig. 1).

Commonly, for modeling the behavior of building materials, local equilibrium between liquid and vapor phase is assumed. In other words, a one-to-one correspondence between local water content and relative humidity is defined at every time step, independently of the process dynamic. According to this assumption, the water retention curve can be obtained through experiments performed at steady state conditions. Commonly employed techniques are the desiccator method [12,13] (for measurements in the hygroscopic range i.e. relative humidity below approximately 95%)

* Corresponding author.
E-mail address: michele.janetti@uibk.ac.at (M. Bianchi Janetti).

Published Journal Article available at: http://dx.doi.org/10.1016/j.ijthermalsci.2016.12.018

Nomenclature

A	specimen surface $[m^2]$
Bi	Biot number $[-]$
c	heat capacity $[J/(kg\,°C)]$
d	specimen thickness $[m]$
D	diffusivity $[m^2/s]$
L	characteristic length $[m]$
Le	Lewis number $[-]$
m	mass $[kg]$
$\dot{m}$	drying rate $[kg/s]$
Nu	Nusselt number $[-]$
p	pressure $[Pa]$
Pr	Prandtl number $[-]$
Re	Reynolds number $[-]$
R	gas constant $[J/(kg\,K)]$
s	standard deviation
T	absolute temperature $[K]$
t	time $[s]$
u	water content $[kg/m^3]$
v	air velocity $[m/s]$
V	specimen volume $[m^3]$
$x; y; z$	coordinates $[m]$
X	parameter Eq. B.5 $[Pa]$
α	heat transfer coefficient $[W/(m^2K)]$
β	mass transfer coefficient $[s/m]$
θ	Celsius temperature [°C]
λ	thermal conductivity $[W/(m\,K)]$
ρ	density $[kg/m^3]$
φ	relative humidity $[-]$

Subscripts

a	air
c	capillary
dry	dry material
f	free saturation
lam	laminar
m	mass transfer
p	constant pressure
sat	saturation
s	surface
$turb$	turbulent
v	vapor
vol	volume
w	liquid water
∞	in the surrounding air

and the pressure plate test [3,13] (for characterization of the super-hygroscopic range).

By applying such steady-state methods, the hysteresis between ad- and desorption, widely studied in previous works (e.g. Ref. [12]), can be observed. However, transient procedures are required in order to investigate the influence of the process dynamic on the material behavior.

Even if the assumption of local equilibrium is common in hygrothermal modeling, recent studies pointed out that, in some cases, it may be quite inaccurate. In Ref. [14], the authors gave experimental evidence of this by carrying out drying, absorption and desorption tests and measuring both water content and relative humidity during time at different positions.

By comparing these results with those obtained at equilibrium conditions through standard techniques, a significant deviation was observed. The measuring equipment employed in that study included different types of sensors and a sophisticated experimental setup: the relative humidity was measured by means of psychrometers (above 96%) and capacitive sensors (below 98%) while the water content was determined through a X-ray projection.

In this study, we propose an alternative method based on non destructive measurements, i.e. infrared thermography and gravimetric analysis. These techniques have been already successfully applied for the assessment of the moisture content in porous building materials in previous works (e.g. Refs. [15–18]). In particular, in Ref. [16] surface temperature measurements are used in combination with gravimetric analysis to determine the transition water content between the super-hygroscopic and hygroscopic range during drying.

In a similar way, in this study the water content and the surface temperature of calcium silicate specimens are measured at different times. Considering that, at least during the early drying period, the water content and temperature inside the specimens are almost uniform, it is possible to determine the transient behavior of the relative humidity trough a mathematical procedure. Hence, the water retention curve can be obtained by linking the relative humidity to the water content.

3. Experimental setup

The experiment consists of drying material samples, previously

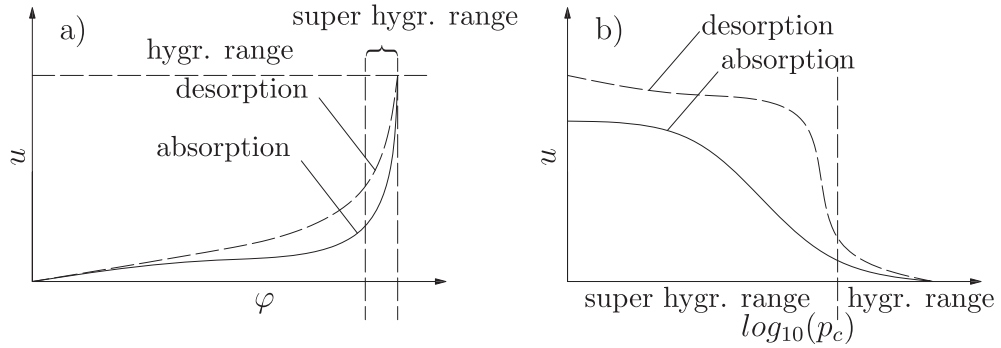

Fig. 1. Water retention curve determined through steady state measurements for absorption and desorption. a) water content versus relative humidity; b) water content versus logarithm of capillary pressure.

doused until the entire pore volume has been filled by liquid water. A preliminary test is carried out in a climatic chamber where the temperature and relative humidity of air are controlled through a ventilation system. Two calcium silicate samples are employed. The experimental setup and the sample schematic are shown in Fig. 2. Note that forced convection is induced and the approaching velocity of air is measured by means of a thermoanemometer. Hence, a nearly constant mass transfer coefficient can be assumed at the sample surface during the whole drying time. The air conditions inside the chamber with their estimated uncertainties and the material properties of the employed calcium silicate samples are reported in Fig. 2 as well.

The mean value of the drying rate is determined by recording the mass loss during time. To this aim, a balance with a repeatability of ± 0.001 $[g]$ is used. The surface temperature of the sample is measured by means of an infrared camera calibrated with respect to known temperatures. The standard deviations of the gravimetric and temperature measurements are reported in Table 1.

In general, the surface temperature and mass loss characterizing the drying of capillary active materials present typical trends. According to previous studies (e.g. Refs. [19–21]), by assuming the initial temperature of the specimen equal to the ambient temperature, the following behavior is expected (see Fig. 3):

- $t < t_1$: Due to evaporation cooling, the temperature decreases steeply determining a reduction of the drying rate. After a certain time ($t = t_1$) the minimum value $\theta(t_1)$ is reached. This stabilization time depends on the heat capacity of the sample and is very short compared to the whole drying period. Indeed, the knowledge of the temperature trend for $t < t_1$ is not required by the method proposed in this study.
- $t_1 < t < t_2$: Both temperature and drying rate remain nearly constant, the first one slightly increasing and the second one slightly decreasing. For the considered experiment it applies $t_2 \approx 46\ h$, as reported in Section 5. This phase determines the characterization of the super hygroscopic range (relative humidity above approximately 95%).
- $t > t_2$: The drying rate decreases dramatically whereas the temperature increases, approximating the surrounding air conditions. During this phase, the hygroscopic range (relative humidity below approximately 95%) is characterized.

4. Mathematical method

The proposed method is based upon a lumped parameter analysis, assuming approximately uniform temperature and water content inside the specimen and at the specimen surface. According to this assumption, it applies:

$$\dot{m}_w(t) = A\beta\left(p_{v,s}(t) - p_{v,\infty}\right) \tag{1}$$

where $\dot{m}_w = dm_w/dt$ represents the drying rate, A the specimen surface and β the convective mass transfer coefficient; $p_{v,s}$ and $p_{v,\infty}$ are the partial pressures of water vapor at the surface and in the surrounding air, respectively.

Taking into account the definition of relative humidity, expressed by Eq. (2):

$$\varphi = \frac{p_v}{p_{sat}} \tag{2}$$

Eq. (1) can be rewritten as follows:

$$\dot{m}_w(t) = A\beta\left(p_{sat,s}(\theta(t))\varphi_s(t) - p_{sat,\infty}\varphi_\infty\right) \tag{3}$$

where $p_{sat,s}$, $p_{sat,\infty}$, φ_s and φ_∞ are the saturation pressure and relative humidity at the surface and in the surrounding air, respectively. Moreover, the saturation pressure p_{sat} can be expressed as a function of the Celsius temperature θ according to the following equation, valid in the temperature range of our interest [22]:

$$p_{sat} = 610.94\, e^{\frac{17.625\ \theta}{243.04+\theta}} \tag{4}$$

Note that all the terms appearing in Eq. (3) except for β and φ_s can be directly measured. Since the air velocity in the chamber is controlled due to ventilation (forced convection), the mass transfer coefficient β can be considered approximately constant during the whole drying period and is calculated as follows:

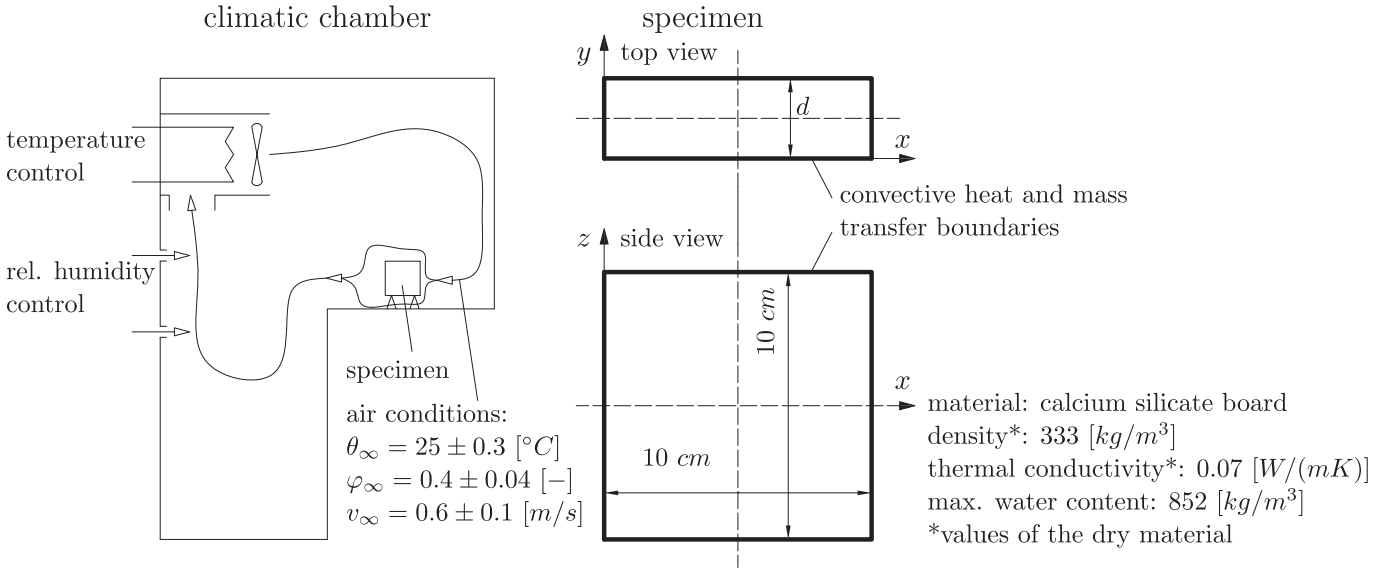

Fig. 2. Climatic chamber, specimen schematic ($d = 3\ cm$) and material properties.

Table 1
Measured surface temperature, relative humidity, water content, drying rate (mean values and standard deviations) and mass transfer Biot number calculated according to Eq. (9).

t	θ	s_θ	φ_s	$\frac{s_{\varphi_s}}{\varphi_s}$	u	$\frac{s_u}{u}$	$\frac{\dot{m}_w}{A}$	$\frac{s_{\dot{m}_w}}{\dot{m}_w}$	Bi_m
$[h]$	$[^\circ C]$	$[K]$	$[-]$	$[\%]$	$\left[\frac{kg}{m^3}\right]$	$[\%]$	$\left[\frac{kg}{m^2\ s}\right]$	$[\%]$	$[-]$
0	–	–	1.0000	–	851.8	0.2	–	–	–
3.8	17.5	0.31	0.9995	4.4	798.1	0.4	3.7E-05	9.1	0.0001
8.5	17.8	0.35	0.9783	6.0	731.9	1.1	3.7E-05	13.8	0.0017
19.6	17.9	0.20	0.9726	4.4	575.2	3.5	3.6E-05	10.7	0.0083
32.1	18.0	0.23	0.9594	8.8	403.2	1.9	3.6E-05	23.8	−0.0008
46.3	17.6	0.29	0.9597	4.1	211.7	15.2	3.4E-05	8.8	−0.001
51.8	18.1	0.69	0.8713	6.5	140.7	19.7	2.7E-05	8.3	0.76
67	22.1	1.08	0.5408	9.8	42.7	31.2	8.9E-06	25.1	5.3703
71	23.0	0.87	0.4885	8.0	34.0	29.6	5.3E-06	38.8	4.6704
73.3	23.1	0.73	0.4788	6.8	29.1	28.1	4.5E-06	41.0	–

$$\beta = \frac{\dot{m}_w(t_1)}{A\left(p_{sat,s}(\theta(t_1))\varphi_s(t_1) - p_{sat,\infty}\varphi_\infty\right)} \tag{5}$$

where $\theta(t_1)$ is the surface temperature after the stabilization phase (see Fig. 3). The relative humidity $\varphi_s(t_1)$ can be assumed with a very good approximation equal to one, as verified in the following section.

Once the mass transfer coefficient has been determined, it is possible to calculate $\varphi_s(t)$ rewriting Eq. (3) as follows:

$$\varphi_s(t) = \frac{\frac{\dot{m}_w(t)}{\beta A} + p_{sat,\infty}\varphi_\infty}{p_{sat,s}(\theta(t))} \tag{6}$$

Finally, the surface water content $u_s(t)$ can be assumed approximately equal to the mean water content inside the specimen $u_{vol}(t)$:

$$u_s(t) \approx u_{vol}(t) = \frac{m_w(t)}{V} \tag{7}$$

where V represents the specimen volume. This assumption applies in case the mass transfer Biot number characterizing the experiment is low enough, as better explained in Section 5.2.

The correlation between water content and relative humidity can be found by linking the values determined through equations (6) and (7) at different times during drying.

Taking into account the Kelvin equation:

$$\varphi = e^{\left(\frac{-p_c}{\rho_w R_v T}\right)} \tag{8}$$

where p_c, ρ_w and R_v are the capillary pressure, the density of liquid water and the gas constant for water vapor, respectively, we are able to express the water content as a function of the capillary pressure: $u = u(p_c)$.

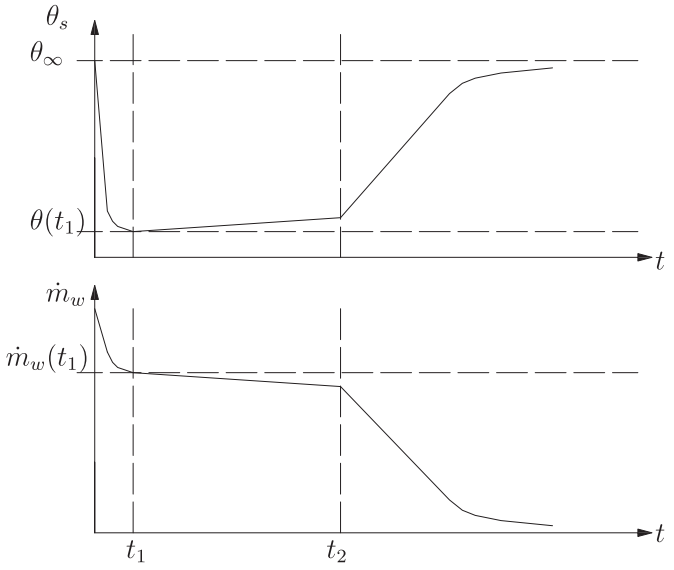

Fig. 3. Typical trends of the mean surface temperature (top) and of the drying rate (bottom) assuming the initial temperature of the specimen equal to the air temperature.

5. Results

In this section the results of the first experimental test described above are discussed. Since the measurements of temperature and water content are not synchronized, the data have been linearly interpolated obtaining the matrix reported in Table 1 (the time-steps refer to the temperature measurements). The uncertainties on the output parameters have been derived according to the error propagation theory, as better described in Section 5.4.

After the determination of the temperature, water content and drying rate, the mass transfer coefficient β has to be estimated. To this aim Eq. (5) is applied, using the surface temperature measured at $t_1 = 3.8$ $[h]$ and assuming with good approximation: $\varphi_s(t_1) \approx 1$. The calculated value is $\beta = (5.1 \pm 0.9)10^{-8}$ $[s/m]$. This result has been verified by determining the Nusselt number for the air flow conditions measured inside the climatic chamber (see Fig. 2) and hence re-calculating the mass transfer coefficient through the empirical equations reported in Appendix A. A value of $\beta = 6.6\ 10^{-8}$ $[s/m]$ has been found, in acceptable agreement with the previous result.

Once the mass transfer coefficient has been determined, the mean relative humidity at the surface can be obtained at each time step through Eq. (6). In Fig. 4a) and b) the measured temperature and relative humidity are reported. The mean water content and the drying rate are shown in Fig. 4c) and d), respectively. Note that the early stabilization phase reported in Fig. 3 can not be observed in these plots since no data are available for $t < t_1$. Indeed, this is not essential for the determination of the water retention curve, which is shown in Fig. 4e) and f) as a function of the relative humidity and logarithm of the capillary pressure, respectively.

5.1. Influence of the boundary conditions

The temperature distribution at the specimen surface for

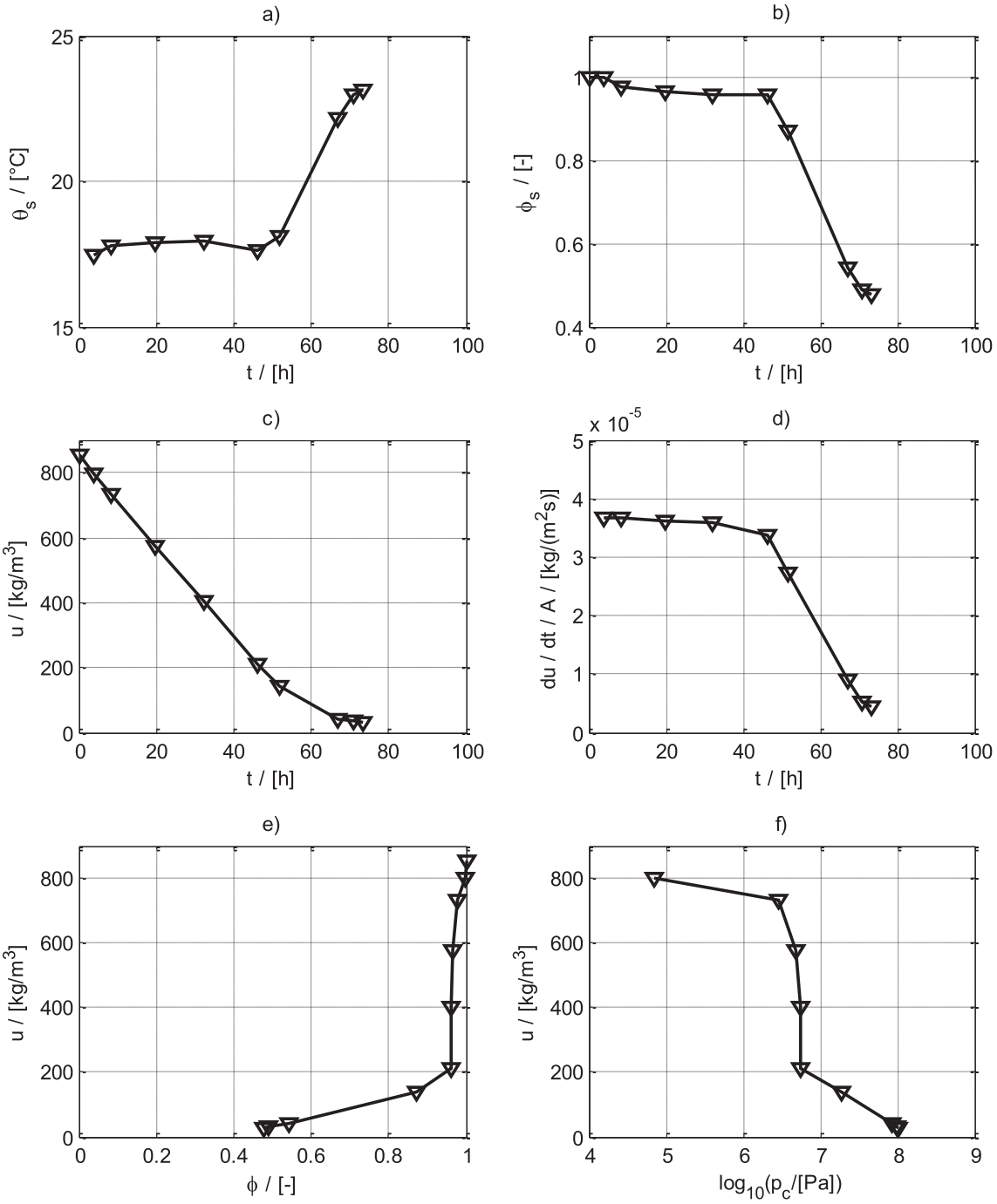

Fig. 4. Trends of a) surface temperature; b) relative humidity; c) water content; d) drying rate; e) and f) water retention curve.

different times can be observed in Fig. 5. These plots show that the temperature is nearly uniform up to approximately 52 [*h*], while differences occur later on between border and center of the specimen. This is due to the fact that evaporation occurs at all boundaries, leading to 3D transfer of heat and mass. Considering this issue, the experiment may be improved by drying the sample just from one side, obtaining in this way one-dimensional transfer and hence uniform surface distributions. This has been investigated through numerical simulation using the hygrothermal model reported in Ref. [21].

An ideal water retention curve is given as model input. Hence, the desorption trend of the water content is re-calculated as a function of the relative humidity, by using the results of the numerical model, according to the method described above in Section 4. The experiment is first reproduced through a 3D model, imposing convective boundary conditions for heat and mass transfer at all boundaries. Then the simulation is repeated for a specimen with ideally adiabatic and sealed borders. In this case, evaporation occurs just at the main surfaces (1D heat and mass transfer through the specimen). By comparing the resulting moisture retention curve with the input function, the influence of all simplifications introduced by the lumped parameter approach is investigated.

In Fig. 6, the trend obtained with the reference specimen (drying

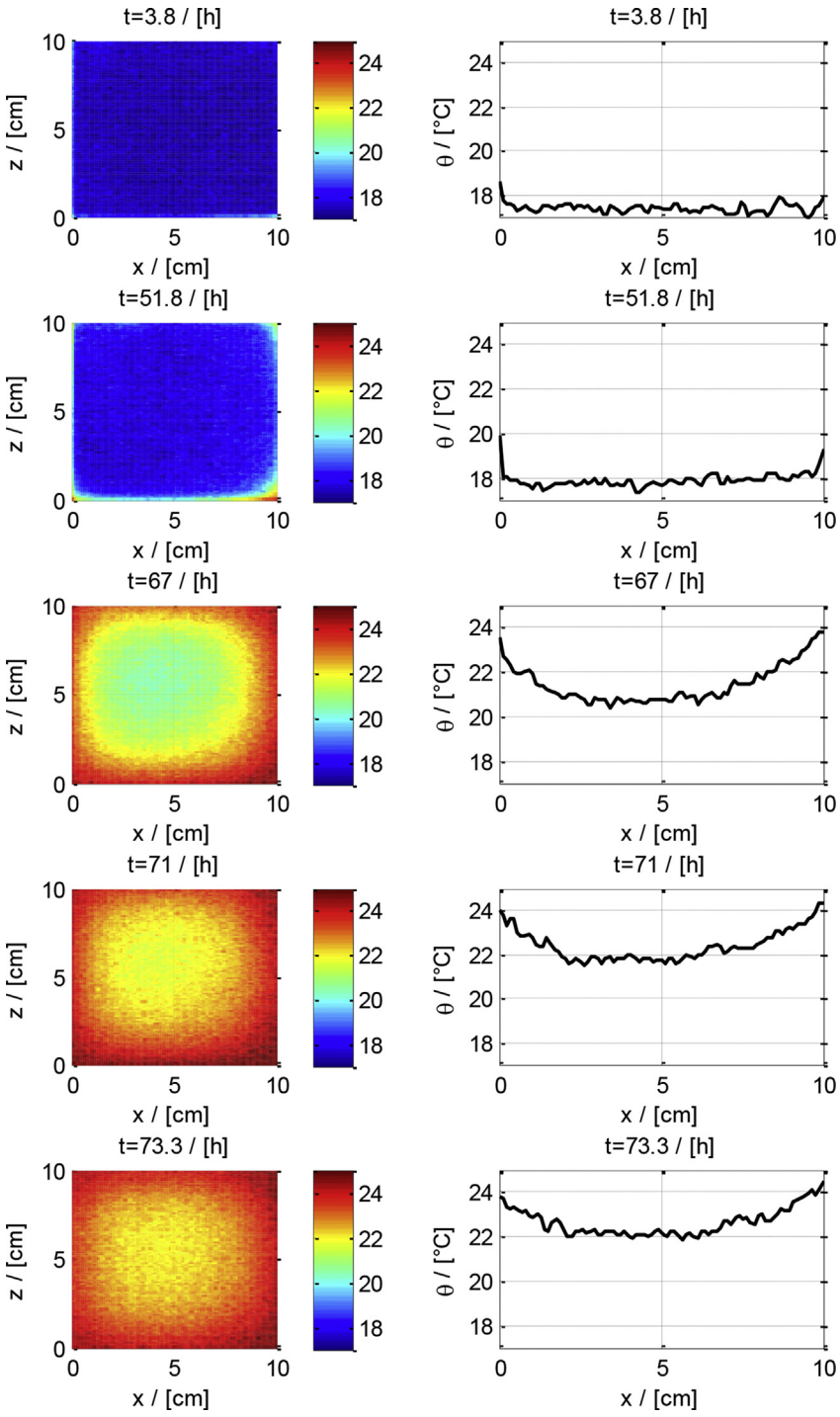

Fig. 5. Left: surface temperature distribution at different times (y = 0; see Fig. 2); Right: temperature profiles at $z = 5$ [cm].

from all boundaries, 3D transfer) is compared with the one resulting from a specimen with adiabatic and sealed borders (1D transfer) and with the exact desorption trend (input function of the simulation). It can be observed that, if 1D drying is imposed, a significant improvement is obtained only in the middle range of capillary pressure ($6 < log_{10}(p_c) < 7.5$), while at high and low capillary pressure the deviation between 3D and 1D results is negligible. Moreover, it has to be considered that applying thermal insulation and sealing material at the border surfaces would make the experimental setup much more complex. In the following section, other simpler measures, which may be applied in order to improve the experiment, are considered.

5.2. *Influence of the specimen's thickness*

The assumption of uniform water content inside the specimen has been verified employing again the numerical model described in Ref. [21].

In Fig. 7 the mean water content at the surface and inside the specimen, as well as the relative difference between these two

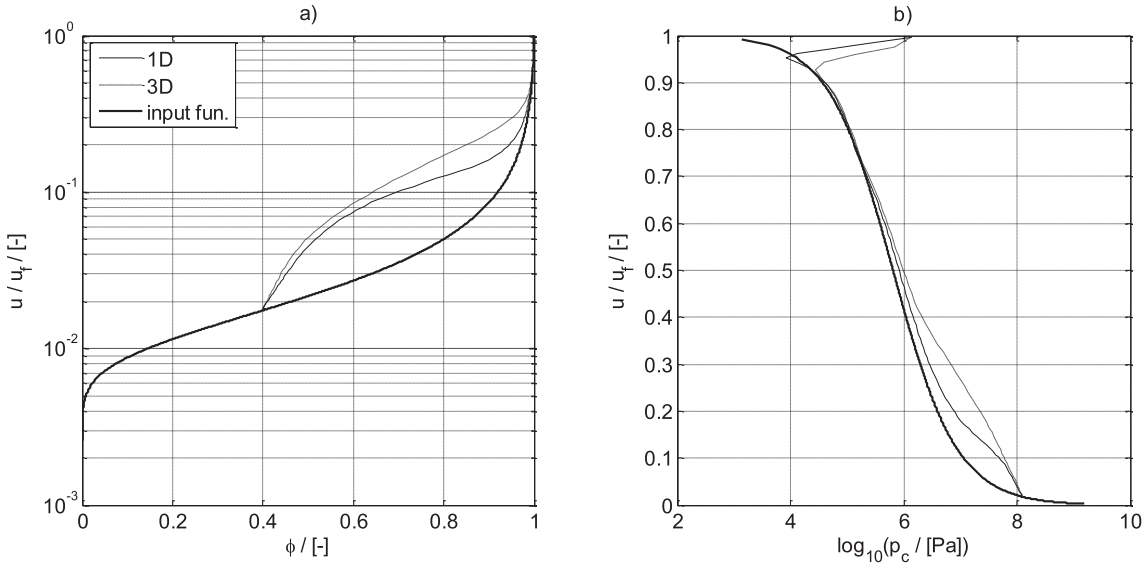

Fig. 6. Comparison between the desorption trend of a sample drying from all boundaries (3D transfer), the one resulting from 1D drying (adiabatic and sealed borders) and the exact trend (input function). a) water content versus relative humidity; b) water content versus logarithm of capillary pressure.

values are reported. It can be observed that first the deviation increases steeper, reaching its maximum value at approximately 60 h. This behavior can be explained taking into account the mass transfer Biot number Bi_m which gives the ratio of the mass transfer resistances inside of and at the surface of the specimen. According to this interpretation, a low Biot number leads to a more homogeneous distribution inside the body.

Considering that in the super-hygroscopic range the capillary transfer of liquid water dominates the mass transfer (hence vapor diffusion is negligible during the early phase of drying), the Biot number can be written as follows:

$$Bi_m = \frac{(V/A)\beta}{\frac{\partial u}{\partial \varphi}\frac{\partial \varphi}{\partial p_v}D_w} \tag{9}$$

where the ratio (V/A) represents the characteristic dimension of the body and the liquid water diffusivity $D_w(u)$ is an increasing function of the water content.

According to Eq. (9), the Biot number increases significantly during drying. Hence, while in the first period almost no difference is observed between surface and internal values, important deviations occur later on.

In Table 1 the values of Bi_m, calculated according to the liquid water diffusivity measured in Ref. [23], are reported. The negative values at $t = 32.1$ $[h]$ and $t = 46.3$ $[h]$ have no physical meaning and can be explained considering that the derivative $\partial u/\partial \varphi$ is negative due to measurement uncertainty in those cases.

According to the above statements, the experiment can be significantly improved by reducing the sample thickness since in this way a lower Biot number and thereby a more uniform moisture distribution is reached. In Fig. 8 the desorption trends obtained through numerical simulation with samples of different dimensions are reported. Similar results can be obtained also by reducing the air velocity in the climatic chamber and hence the

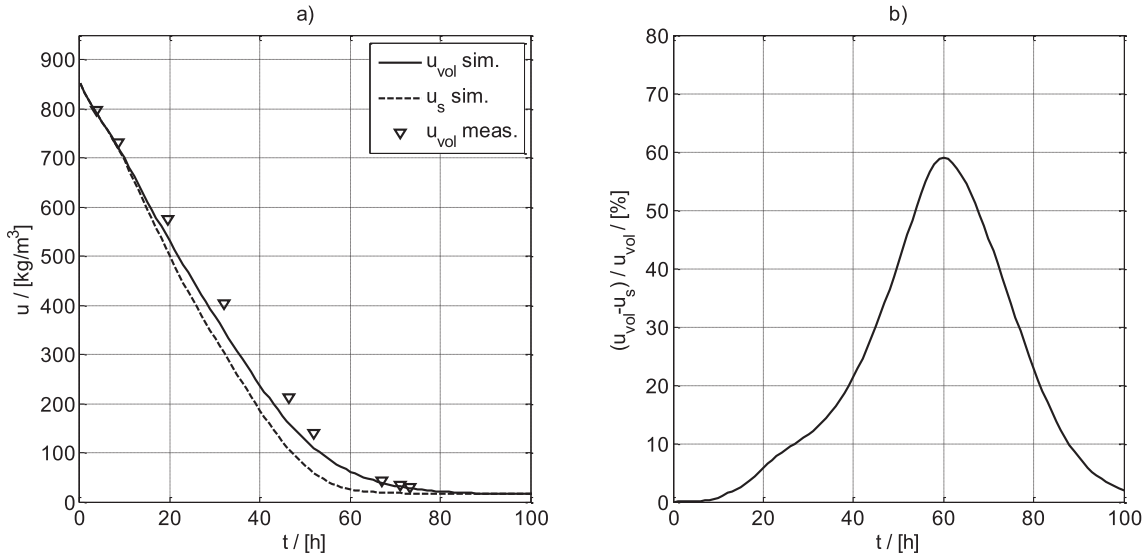

Fig. 7. a) mean value of the water content at the specimen surface (u_s) and inside the specimen (u_{vol}); b) deviation between volume and surface values.

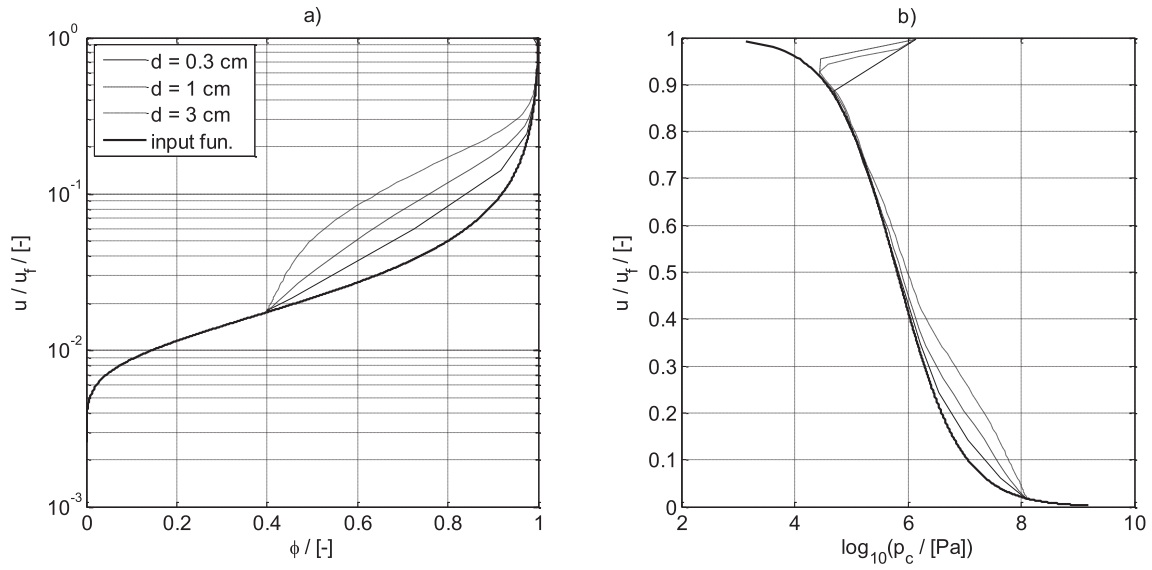

Fig. 8. Comparison between the trends obtained with samples of different thickness (3D transfer) and the exact trend (input function). The trends have been obtained through numerical simulation according to the model reported in Ref. [21]. a) water content versus relative humidity; b) water content versus logarithm of capillary pressure.

mass transfer coefficient β. However, this measure is limited by the fact that forced convection is required, in order to guarantee a nearly constant mass transfer coefficient during the whole drying time and all-over the specimen surface.

5.3. Comparison with other measured data

In Fig. 9 the water retention curve obtained through the drying test is compared with values determined by means of the desiccator method for absorption and desorption in the hygroscopic range. For better accuracy, the drying trend has been corrected by reducing the water content according to the numerical results reported in Fig. 7 b). It can be observed that, in accordance with the considerations made above, the errors due to non-uniform distribution are important just at low water content.

The values measured at steady state conditions are interpolated through the mathematical model proposed by Ref. [24]; however, since no data are available in the super hygroscopic range, the reported trends may be inaccurate in this region.

Further verification is carried out by comparing the results of this study with those published by Janssen et al. [14] (see Fig. 10). Despite some deviation at high and low water content which may be given by material differences, a rather good agreement is observed.

5.4. Random uncertainties

The standard deviations of the measured temperature, water content and drying rate as well as the resulting uncertainties on the relative humidity at different times are reported in Table 1, while the uncertainties affecting the boundary conditions and the accuracy of the employed instrumentation are reported in Section 3. The

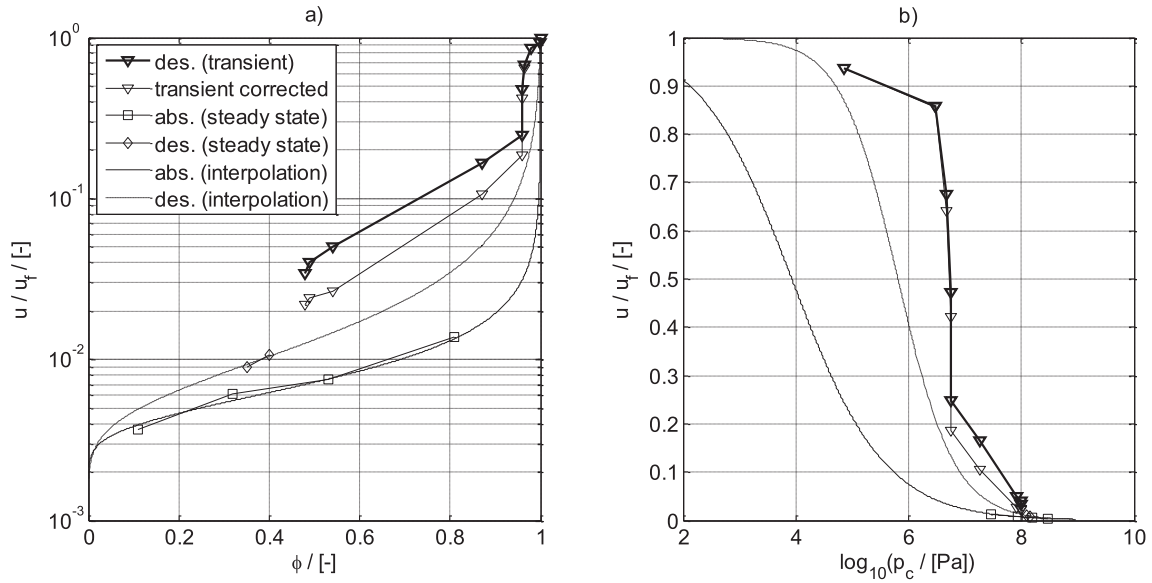

Fig. 9. Results of the drying test (transient) compared with those obtained by means of the desiccator method (steady state). a) water content versus relative humidity; b) water content versus logarithm of capillary pressure. The corrected values are obtained by reducing the water content according to the results reported in Fig. 7 b).

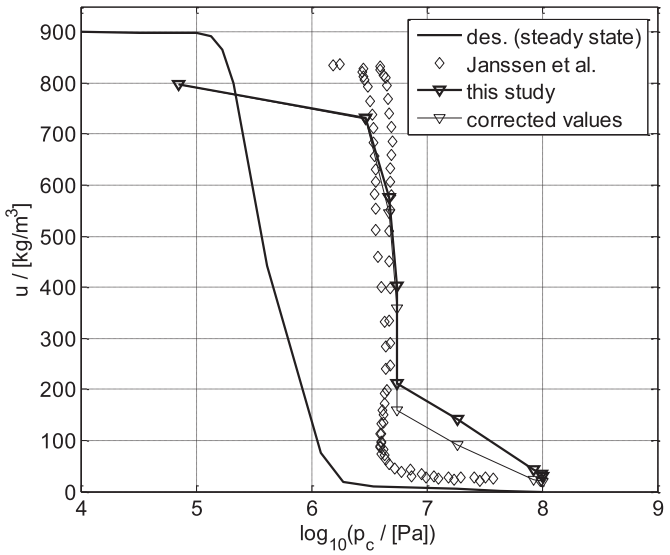

Fig. 10. Comparison between the results of this study and measurements by Janssen et al. [14]. The corrected values are obtained by reducing the water content according to the results reported in Fig. 7 b).

resulting random uncertainties have been estimated according to the error propagation theory by means of the equations reported in Appendix B.

Note that these values are rather high and a better measurement precision has to be achieved. Such improvement is realistic, considering the accuracy of the up-to-date instrumentation. In particular the gravimeter analysis can be improved and the uncertainty on the infrared measurements can be reduced using a more accurate camera. Important uncertainties are given by oscillations of the temperature, relative humidity and velocity of air, as well as by non exactly uniform conditions inside the climatic chamber. With regard to these issues, there is room for significant improvement.

Moreover, considering that the actual values have been obtained employing only two samples, further tests have to be carried out for a more representative statistics.

6. Conclusions and outlook

This study describes a new procedure to determine the water retention curve of porous capillary active materials through transient drying tests.

The proposed method is less time consuming and differs significantly from other ones based on experiments at steady state conditions. Moreover, it is suitable for investigation of the so called dynamic effects which may affect the moisture storage behavior of porous building materials. Such effects have been observed in a recent study by Janssen et al. [14] employing a more sophisticated equipment.

A preliminary test performed with the new method on calcium silicate specimens gave promising results, showing a good agreement with the values found by Ref. [14].

The experiment may be improved by reducing the characteristic mass transfer Biot number, since this leads to more uniform temperature and moisture distribution inside the specimen. Hence, the test can be optimized by reducing the sample dimension and the convective mass transfer coefficient (lower air velocity). On the other hand, the method presented in this paper may not be applicable to materials with very low liquid water diffusivity.

For a better definition of the applicability range of the method and for obtaining representative statistics, further tests with different materials and boundary conditions are required.

Acknowledgments

The authors kindly thank Renato Passaniti, Dominik Granig, Andreas Saxer, Markus O. Feichter and Marco Romani for their support and remarks.

Appendix A

Empirical equations for calculation of heat and mass transfer coefficients, valid for $10 < Re < 10^7$ and $0.6 < Pr < 1000$ [25]:

$$\alpha = \frac{Nu\lambda_a}{L} \tag{A.1}$$

$$\beta = \frac{1}{R_v T}\frac{\alpha}{\rho_a c_{p,a}} Le^{-\frac{2}{3}} \tag{A.2}$$

$$Nu = 0.3 + \left(Nu_{lam}^2 + Nu_{turb}^2\right)^{1/2} \tag{A.3}$$

$$Nu_{lam} = 0.664 Re^{1/2} Pr^{1/3} \tag{A.4}$$

$$Nu_{turb} = \frac{0.037 Re^{0.8} Pr}{1 + 2.443 Re^{-0.1}\left(Pr^{2/3} - 1\right)} \tag{A.5}$$

all symbols in equation (A.1)–(A.5) are clarified in the nomenclature. According to [25], it has been assumed $Le = 0.87$.

Appendix B

Equations for calculation of the random uncertainties, derived according to the error propagation theory by considering independent input variables (covariance equal to zero):

$$\left(\frac{s_\beta}{\beta}\right)^2 \approx \left(\frac{s_{\dot m_w}}{\dot m_w}\right)^2 + \frac{\left(p_{sat,s}\varphi_s\right)^2\left(\left(\frac{s_{p_{sat,s}}}{p_{sat,s}}\right)^2 + \left(\frac{s_{\varphi_s}}{\varphi_s}\right)^2\right)}{\left(p_{sat,s}\varphi_s - p_{sat,\infty}\varphi_\infty\right)^2} + \frac{\left(p_{sat,\infty}\varphi_\infty\right)^2\left(\left(\frac{s_{p_{sat,\infty}}}{p_{sat,\infty}}\right)^2 + \left(\frac{s_{\varphi_\infty}}{\varphi_\infty}\right)^2\right)}{\left(p_{sat,s}\varphi_s - p_{sat,\infty}\varphi_\infty\right)^2} \tag{B.1}$$

$$\left(\frac{s_{p_{sat}}}{p_{sat}}\right)^2 \approx \left(\frac{17.625\,\theta}{243.04 + \theta}\right)^2\left(\frac{s_\theta^2}{\theta^2} + \frac{s_\theta^2}{(243.04 + \theta)^2}\right) \tag{B.2}$$

$$\left(\frac{s_{\varphi_s}}{\varphi_s}\right)^2 \approx \left(\frac{s_X}{X}\right)^2 + \left(\frac{s_{p_{sat,s}}}{p_{sat,s}}\right)^2 \tag{B.3}$$

$$\left(\frac{s_X}{X}\right)^2 \approx \frac{\left(\frac{\dot{m}_w}{\beta A}\right)^2 \left(\left(\frac{s_{\dot{m}_w}}{\dot{m}_w}\right)^2 + \left(\frac{s_\beta}{\beta}\right)^2\right)}{\left(\frac{\dot{m}_w}{\beta A} + p_{sat,\infty}\varphi_\infty\right)^2} + \frac{\left(p_{sat,\infty}\varphi_\infty\right)^2 \left(\left(\frac{s_{p_{sat,\infty}}}{p_{sat,\infty}}\right)^2 + \left(\frac{s_{\varphi_\infty}}{\varphi_\infty}\right)^2\right)}{\left(\frac{\dot{m}_w}{\beta A} + p_{sat,\infty}\varphi_\infty\right)^2} \quad \text{(B.4)}$$

$$X = \frac{\dot{m}_w}{\beta A} + p_{sat,\infty}\varphi_\infty \quad \text{(B.5)}$$

References

[1] Feist W. "Passivhauskomponenten und Innendämmung," Protokollband Nr.32. Faktor 4 auch bei sensiblen Altbauten: Passivhauskomponeneten + Innendämmung. Darmstadt; 2005. p. 1–16.

[2] Künzel H, Kiessl K. Calculation of heat and moisture transfer in exposed building components. Int J Heat Mass Transf oct 1996;40:159–67.

[3] Krus M. Moisture transport and storage coefficients of porous mineral building materials - theoretical principles and new test methods. Fraunhofer IRB Verlag Stuttgart; 1996, ISBN 3-8167-4535-0.

[4] Häupl P, Grunewald J, Fechner H, Stopp H. Coupled heat air and moisture transfer in building structures. Int J Heat Mass Transf 1997;40(7):1633–42.

[5] Baggio P, Bonacina C, Shrefler BA. Some considerations on modeling heat and mass transfer in porous media. Transp Porous Media 1997;28:233–51.

[6] Grunewald J. Diffusiver und konvektiver Stoff- und Energietransport in kapillarporösen Baustoffen. PhD thesis. Technischen Universität Dresden; 1997.

[7] Häupl P, Fechner H. Hygric material properties of porous building materials. J Build Phys 2003;26(3):259–84.

[8] van Schijndel AWM. Integrated modeling of dynamic heat, air and moisture processes in buildings and systems using SimuLink and COMSOL. Build Simul 2009;2:143–55.

[9] Traoré I, Lacroix D, Trovalet L, Jeandel G. Heat and moisture transport in wooden multi-composite panels. Dynamic study of the air layer impact on the building envelope energetic behavior. Int J Therm Sci 2011;50(11):2290–303.

[10] Roels S, Carmelit J, Hens H, Adan O, Brocken H, Cerny R, et al. Interlaboratory Comparison of hygric properties of porous building materials. J Therm Envelop. Build Sci 2004;27:307–25.

[11] Ebert HP, Hemberger F. Intercomparison of thermal conductivity measurements on a calcium silicate insulation material. Int J Therm Sci 2011;50(10): 1838–44.

[12] Scheffler GA. Validation of hygrothermal material modelling under consideration of the hysteresis of moisture storage. PhD thesis. Technischen Universität Dresden; 2008.

[13] Feng C, Janssen H, Feng Y, Meng Q. Hygric properties of porous building materials: analysis of measurement repeatability and reproducibility. Build Environ 2015;85:160–72.

[14] Janssen H, Scheffler GA, Plagge R. Experimental study of dynamic effects in moisture transfer in building materials. Int J Heat Mass Transf 2016;98:141–9.

[15] Baggio P, Bonacina C, Grinzato E, Bison P, Bressan C. Non-destructive tests for measurement of moisture content in porous building materials. Theoretical and experimental approach. Conserv. stone other Mater Proc Int RILEM/ UNESCO Congr 1993;1:252–9.

[16] TavukçuoÄŸlu A, Grinzato E. Determination of critical moisture content in porous materials by IR thermography. Quant. InfraRed Thermogr J 2006;3(2): 231–45.

[17] Furmański P, Wiśniewski T, Wyszyńska E. Detection of moisture in porous materials through infrared methods. Arch. Thermodyn 2008;29(1):19–40.

[18] Barreira E, Almeida RMSF, Delgado JMPQ. Infrared thermography for assessing moisture related phenomena in building components. Constr Build Mater 2016;110:251–69.

[19] Krischer O. In: auf zweite, editor. Die wissenschaftlichen Grundlagen der Trocknungstechnik. Berlin: Springer-Verlag; 1963.

[20] Paepcke A, Nicolai A. Alternating direction implicit methoden für die Bauteilsimulation: Chancen und Herausforderungen. Berlin: BAUSIM; 2012. p. 133–9.

[21] Bianchi Janetti M, Ochs F, Colombo LPM. Hygrothermal modeling: a numerical and experimental study on drying. Comsol Conference München. 2016.

[22] Alduchov OA, Eskridge RE. Improved Magnus form approximation of saturation vapor pressure. J Appl Meteor 1995;35:601–9.

[23] Bianchi Janetti M, Carrubba TA, Ochs F, Feist W. Heat flux measurements for determination of the liquid water diffusivity in capillary active materials. Int J Heat Mass Transf 2016;97:954–63.

[24] Holm A, Krus M, Künzel H. Approximation der Feuchtespeicherfunktion aus einfach bestimmbaren Kennwerten. IBP-Mitteilung 406 2002;29:10–1.

[25] Baehr HD, Stephan K. Wärme- und Stoffübertr. sixth ed. Berlin: Springer-Verlag; 2008.